Proc. Natl. Acad. Sci. USA
Vol. 92, pp. 10272–10276, October 1995
Neurobiology

Calcium signaling in a narrow somatic submembrane shell during synaptic activity in cerebellar Purkinje neurons

(cerebellum/confocal microscopy/synaptic transmission)

J. EILERS*, G. CALLEWAERT†, C. ARMSTRONG‡, AND A. KONNERTH*§

*I. Physiologisches Institut, Universität des Saarlandes, 66421 Homburg, Germany; †Laboratory of Physiology, University of Leuven, 3000 Leuven, Belgium; and ‡Department of Physiology, University of Pennsylvania, Philadelphia, PA 19104

Contributed by C. Armstrong, July 14, 1995

ABSTRACT **Temporal and spatial changes in the intracellular Ca^{2+} concentration ($[Ca^{2+}]_i$) were examined in dendrites and somata of rat cerebellar Purkinje neurons by combining whole-cell patch-clamp recording and fast confocal laser-scanning microscopy. In cells loaded via the patch pipette with the high-affinity Ca^{2+} indicator Calcium Green-1 ($K_d \approx 220$ nM), a single synaptic climbing fiber response, a so-called complex spike, resulted in a transient elevation of $[Ca^{2+}]_i$ that showed distinct differences among various subcellular compartments. With conventional imaging, the Ca^{2+} signals were prominent in the dendrites and almost absent in the soma. Confocal recordings from the somatic region, however, revealed steep transient increases in $[Ca^{2+}]_i$ that were confined to a submembrane shell of 2- to 3-μm thickness. In the central parts of the soma $[Ca^{2+}]_i$ increases were much slower and had smaller amplitudes. The kinetics and amplitudes of the changes in $[Ca^{2+}]_i$ were analyzed in more detail by using the fast, low-affinity Ca^{2+} indicator Calcium Green-5N ($K_d \approx 17$ μM). We found that brief depolarizing pulses produced $[Ca^{2+}]_i$ increases in a narrow somatic submembrane shell that resembled those seen in the dendrites. These results provide direct experimental evidence that the surface-to-volume ratio is a critical determinant of the spatiotemporal pattern of Ca^{2+} signals evoked by synaptic activity in neurons.**

Many postsynaptic events are controlled by changes in the concentration of intracellular Ca^{2+} ($[Ca^{2+}]_i$). Thus, it is well established that various forms of synaptic plasticity, including long-term potentiation (for review, see ref. 1), long-term depression (2, 3), and rebound potentiation of inhibitory synapses (4), are initiated by a transient increase in $[Ca^{2+}]_i$. An understanding of how intracellular Ca^{2+} ions act requires precise information on both the temporal and spatial aspects of such synaptically induced Ca^{2+} signals (5).

In cerebellar Purkinje neurons, large and fast Ca^{2+} signals found in dendrites contrast with much smaller and slower Ca^{2+} signals seen in the cell bodies (2, 6–9). It has been suggested that the small amplitude of the somatic Ca^{2+} signals is the result of the heterogeneous distribution of voltage-operated Ca^{2+} channels with a low density in the somatic region compared to the dendrites (8, 10). This view was also supported by immunohistochemical data indicating that P-type Ca^{2+} channels, the predominant Ca^{2+} channel type in cerebellar Purkinje neurons, are particularly abundant in the dendrites but are not abundant in the somata (11, 12). Recent voltage-clamp studies, however, demonstrated that depolarizing steps associated with large Ca^{2+} currents also invariably cause large increases in $[Ca^{2+}]_i$ in the somata of Purkinje neurons (ref. 13; M. Kano, A. Verkhratsky, R. Schneggenburger, and A.K., unpublished work). In the present study we used a confocal laser-scanning system with a fast acquisition rate (60 Hz–1 kHz) to investigate the spatial distribution of activity-dependent changes in $[Ca^{2+}]_i$ in rat cerebellar Purkinje neurons. The results show that even single synaptic climbing fiber (CF)-mediated responses produce spike-like increases in $[Ca^{2+}]_i$ not only in dendrites but also in a narrow somatic submembrane shell.

MATERIALS AND METHODS

Experiments were done on Purkinje neurons in 200-μm-thick cerebellar slices obtained from 6- to 26-day-old rats ($n = 18$) and adult mice ($n = 7$). The slices were prepared and maintained as described (14). During experiments, slices were continuously perfused with a solution containing 125 mM NaCl, 2.5 mM KCl, 2 mM $CaCl_2$, 1 mM $MgCl_2$, 1 mM NaH_2PO_4, 26 mM $NaHCO_3$, 20 mM glucose, 20 μM bicuculline (pH 7.3), equilibrated with 95% O_2/5% CO_2. All experiments were done at room temperature (21–23°C). Tight-seal somatic recordings were obtained from Purkinje neurons with an EPC-9 patch-clamp amplifier (HEKA Electronics, Lambrecht, Germany) using pipettes with 1.5- to 2.5-MΩ resistance. Afferent CFs were activated with a stimulation pipette placed in the granule cell layer (14, 15). Ca^{2+} signals were recorded under either current-clamp conditions during CF stimulation or voltage-clamp conditions during depolarizing voltage steps. For current-clamp recordings, the pipette solution contained 140 mM KCl, 4 mM MgATP, 0.4 mM Na_3GTP, 10 mM Hepes, and 0.5 mM Calcium Green-1 (Molecular Probes). For most voltage-clamp recordings slices were taken from 6- to 8-day-old rats. At this age, the dendritic tree of Purkinje neurons is not fully developed (see Fig. 3), allowing better voltage control (13, 15). In these experiments the pipette solution contained 140 mM CsCl, 4 mM MgATP, 0.4 mM Na_3GTP, 10 mM tetraethylammonium chloride, 10 mM Hepes, 0.5 mM Calcium Green-5N (Molecular Probes), and, in addition, 500 nM tetrodotoxin (Sigma) was added to the bath solution.

Fluorometric Ca^{2+} measurements were done by using a confocal laser-scanning system (Odyssey, Noran Instruments, Middleton, WI) mounted on an upright microscope (Axioplan, Zeiss) equipped with water-immersion objectives (Achroplan, Zeiss; ×63, numerical aperature 0.9 and ×40, numerical aperature 0.75). To assure that the standard image-acquisition-rate 30 Hz (60 Hz frame rate after off-line de-interlacing) was adequate for resolving the time course of the transient Ca^{2+} changes, the fluorescence changes were also acquired in the line-scanning mode at a rate of 15.75 kHz. Line-scan data were then filtered at 1 kHz by placing adjacent values in bins. Further methodological details can be found elsewhere (16).

The publication costs of this article were defrayed in part by page charge payment. This article must therefore be hereby marked "*advertisement*" in accordance with 18 U.S.C. §1734 solely to indicate this fact.

Abbreviations: CF, climbing fiber; $[Ca^{2+}]_i$, intracellular Ca^{2+} concentration; $\Delta F/F$, increase in fluorescence divided by baseline fluorescence.

§To whom reprint requests should be addressed.

All fluorescence data are expressed as the increase in fluorescence divided by baseline fluorescence ($\Delta F/F$). The dissociation constants (K_d) of Calcium Green-1 and Calcium Green-5N were estimated *in vitro* by using Ca^{2+} calibration kits (Molecular Probes) and were ≈220 nM and 17 μM, respectively, for the present experimental conditions. We estimated that for resting conditions a 100% increase in $\Delta F/F$ of Calcium Green-5N corresponded to an increase in $[Ca^{2+}]_i$ of ≈400 nM.

RESULTS

Synaptic CF Stimulation. Stimulation of the afferent CF excites each Purkinje neuron, giving rise to a complex spike—i.e., a large depolarization causing a burst of action potentials (Fig. 1*C*). When cells were loaded with the high-affinity Ca^{2+} indicator Calcium Green-1 (Fig. 1*A*), transient changes in $[Ca^{2+}]_i$ could be detected during a single complex spike. By using nonconfocal imaging microscopy, a clear Ca^{2+} transient was recorded in both the proximal and distal dendritic area while the $[Ca^{2+}]_i$ in the soma changed very little (Fig. 1*B*, traces 1–3). The Ca^{2+} transient in the distal dendrite peaked ≈35 ms after CF activation, a time coinciding with the end of the complex spike, and then slowly decayed to basal level (trace 1). The time course of Ca^{2+} decay was best fitted with two exponentials with time constants of ≈0.2 s and 0.8 s, respectively. The Ca^{2+} transient recorded in the proximal dendrite had a similar time course, but its peak amplitude was about half that recorded in the distal part (trace 2). The somatic Ca^{2+} signal was about one-tenth of that recorded in the proximal dendritic signal and had a much slower rise time (trace 3). Assuming a resting $[Ca^{2+}]_i$ of 25–40 nM, as determined under similar experimental conditions in experiments using fura-2 (17), we estimate a peak rise in $[Ca^{2+}]_i$ in the distal dendrite of well over 150 nM.

Fig. 2 shows the confocal image of a soma of a Purkinje neuron together with the time course of somatic $[Ca^{2+}]_i$ changes in response to a single CF stimulation. Although somatic Ca^{2+} signals were barely detectable in the nonconfocal mode (Fig. 1), confocal imaging allowed us to resolve a clear and fast Ca^{2+} transient in the soma. This fast Ca^{2+} signal was, however, not seen throughout the whole soma but was spatially restricted to a subplasmalemmal shell. Just underneath the membrane, $[Ca^{2+}]_i$ increased rapidly and reached its peak amplitude within ≈50 ms (Fig. 2*B*, left trace)—that is, at the end of the complex spike. The Ca^{2+} transient in this subplas-

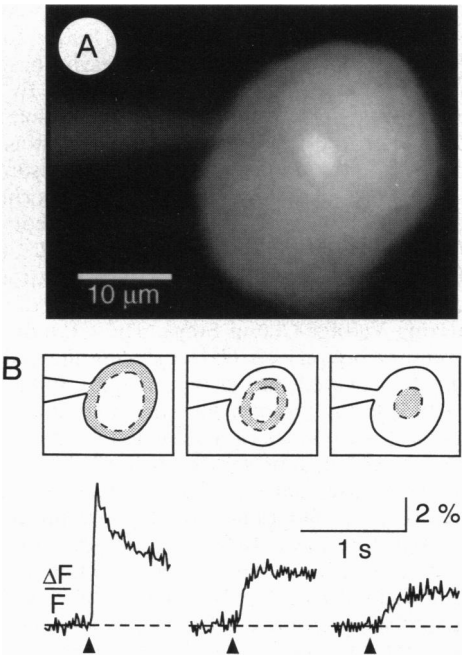

FIG. 2. Intrasomatic pattern of Ca^{2+} signals evoked by CF stimulation. (*A*) Confocal fluorescence image of the soma of a Purkinje neuron loaded with Calcium Green-1 via the patch pipette. (*B*) (*Lower*) Ca^{2+} transients in a submembrane shell (*Left*), an intermediate shell (*Middle*), and the central region (*Right*) of the soma evoked by CF stimulation. (*Upper*) The different somatic regions are schematically illustrated. The width of the submembrane shell was ≈3 μm. The electrical synaptic response associated with these Ca^{2+} signals was similar to that shown in Fig. 1*C*.

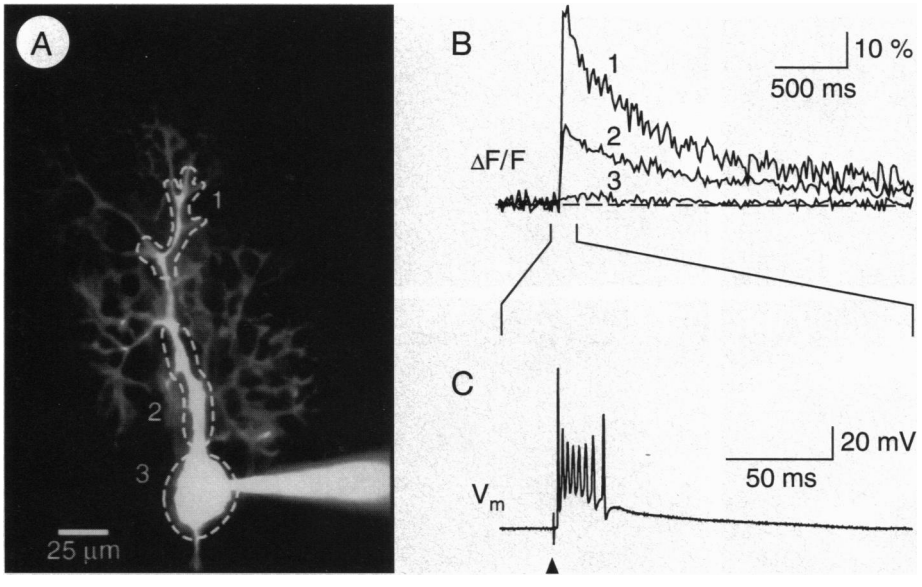

FIG. 1. Ca^{2+} signals associated with a single CF-mediated synaptic response in a current-clamped cerebellar Purkinje neuron. (*A*) Fluorescence image of a Purkinje neuron loaded with the calcium indicator Calcium Green-1 via the patch pipette. Dashed lines mark two dendritic regions (regions 1 and 2) and a somatic region (region 3) from which fluorescence was measured. (*B*) Ca^{2+} transients in dendritic (traces 1 and 2) and somatic (trace 3) regions evoked by a single CF stimulation (numbers correspond to regions in *A*). Fluorescence signals were acquired in the nonconfocal mode by fully opening the aperture of the confocal recording system. (*C*) Corresponding excitatory postsynaptic response (or complex spike) evoked by CF stimulation. Membrane potential (V_m) was −65 mV. Here and in Fig. 2 arrowheads mark the time points of a single synaptic stimulation.

malemmal shell decayed in two phases: an early phase lasting for ≈500 ms was followed by a late phase lasting for several seconds (only partially shown). During the early phase, $[Ca^{2+}]_i$ rapidly decayed to <50% of the peak amplitude. By contrast, the CF-induced rise in $[Ca^{2+}]_i$ at the innermost somatic shell was much smaller and slower; peak amplitude was reached after ≈500 ms (Fig. 2*B*, right trace). For comparison, the size and time course of the Ca^{2+} signal in this innermost shell would match that observed in the soma using conventional imaging (Fig. 1*B*, trace 3). Thus, the CF-induced Ca^{2+} transient is not an exclusive property of the dendritic tree but can be readily observed in the subplasmalemmal shell of the soma.

Depolarizing Voltage-Clamp Steps. The CF-induced Ca^{2+} transient presumably reflects Ca^{2+} entering the cell through Ca^{2+} channels activated during the complex spike response (2–4, 18, 19). The finding of a somatic spike-like Ca^{2+} transient, therefore, is evidence of a somatic localization of voltage-dependent Ca^{2+} channels in cerebellar Purkinje neurons. To allow more precise control of Ca^{2+} influx via this pathway, we recorded $[Ca^{2+}]_i$ changes under voltage-clamp conditions. We also used the low-affinity Ca^{2+} indicator Calcium Green-5N to reduce the effect of exogenous buffer on the amplitude and kinetics of the Ca^{2+} signal (20). Fig. 3 shows a series of confocal images taken from the soma and proximal part of the dendritic tree of a Purkinje neuron. Each image frame corresponds to a time period of 33 ms. At the time indicated by the white flag (second image), the cell was depolarized from a holding potential of −60 mV to 0 mV for 100 ms. The depolarization produced the expected dendritic Ca^{2+} transient and a clear peripheral ring of high $[Ca^{2+}]_i$ in the soma of the cell. During the depolarizing step, there was a rapid buildup of $[Ca^{2+}]_i$ in the subplasmalemmal region, which reached a peak level at the end of the depolarizing pulse (see also Fig. 4). After the peak, $[Ca^{2+}]_i$ slowly decayed to control levels. Fig. 4*A* shows the Ca^{2+} transient in three different cellular regions. $[Ca^{2+}]_i$ in the proximal dendrite (*Left*, dendrite) rapidly increased during the depolarizing step, reached its maximum at the end of the depolarizing pulse, and then slowly recovered with a time constant of ≈0.7 s. In the somatic region (*Right*, soma), Ca^{2+} signals were heterogeneous. In the subplasmalemmal region (trace a) there was a clear Ca^{2+} transient with a maximum at the end of the depolarization. After the peak, the $[Ca^{2+}]_i$ in the submembrane shell decayed to basal levels in two phases: a fast component with a time constant of ≈0.1 s was followed by a second slow component with a time constant of ≈0.8 s (only partially shown). In contrast to the subplasmalemmal shell, the Ca^{2+} signal in the central somatic region (trace b) had a much smaller amplitude and a slower rise time, and the decay phase was apparently monophasic with a time constant of ≈1 s. The $[Ca^{2+}]_i$ gradient that developed between the central and the submembrane region could be observed for ≈700 ms. At later times, $[Ca^{2+}]_i$ was uniformly distributed throughout the soma. The line-scan data shown in Fig. 4*B* (gray trace) were acquired in the same submembrane region at a frequency of 1 kHz and show that the peak and the time course of the Ca^{2+} signals acquired at 60 Hz (solid trace) were measured reliably.

These observations were not restricted to the early postnatal stages of development. Similar somatic $[Ca^{2+}]_i$ gradients in response to depolarizing pulses were also observed in all Purkinje neurons tested from rats up to an age of 26 days, as well as in Purkinje neurons from adult mice.

DISCUSSION

As in previous studies (2, 4, 6–10), nonconfocal imaging showed that synaptic CF stimulation caused a large transient rise in $[Ca^{2+}]_i$ in all parts of the dendritic tree but apparently not in the somatic region. A low density of Ca^{2+} channels in the soma would explain this result. In favor of this hypothesis, immunohistochemical data suggested that P-type Ca^{2+} channels are particularly abundant in dendrites of Purkinje neurons but are not abundant in the somata (11, 12). Recent fluorometric measurements, however, revealed depolarization-induced Ca^{2+} transients in the somata of Purkinje neurons (ref. 13; M. Kano, A. Verkhratsky, R. Schneggenburger, and A.K., unpublished work). Using fast laser-scanning confocal imaging, we found that Ca^{2+} transients were present even during single synaptic CF stimulation in both the soma and the dendritic tree. The somatic rise in $[Ca^{2+}]_i$ was initially restricted to a region just underneath the surface membrane, giving rise to a peripheral ring of high $[Ca^{2+}]_i$. Because of

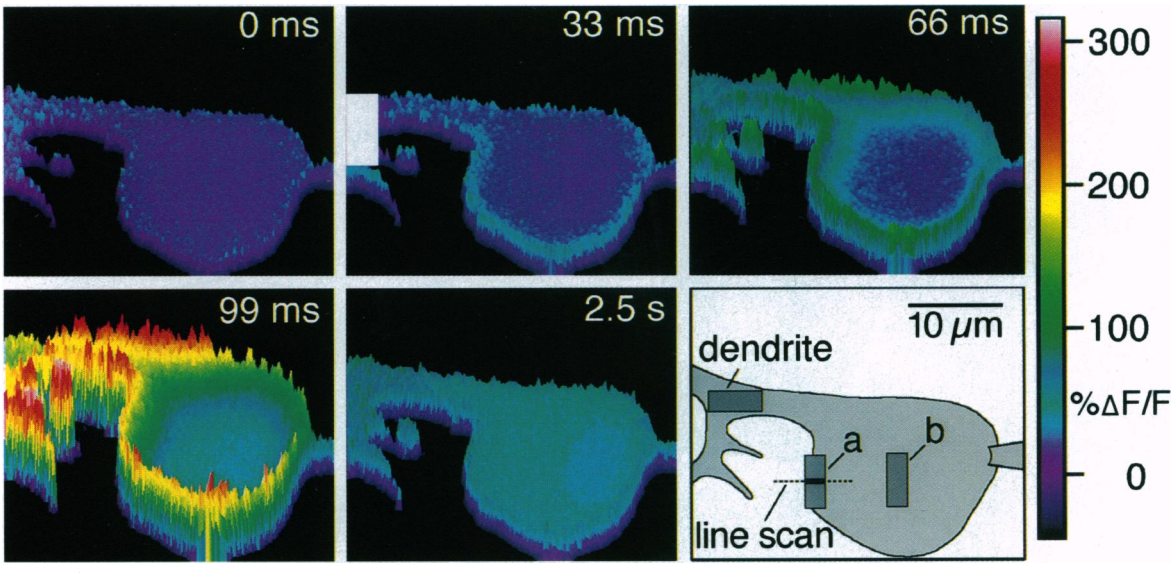

FIG. 3. Spatial distribution of Ca^{2+} signals in a voltage-clamped Purkinje neuron from a 6-day-old rat. Sequence of pseudocolor confocal fluorescence images of a Purkinje neuron loaded with Calcium Green-5N via the patch pipette and depolarized for 100 ms from −60 mV to 0 mV. Each image represents a single frame acquired at video rate (30 Hz) at times indicated at top right corners. The start of the depolarizing step is indicated by the white flag in the second image. The peak increases in $[Ca^{2+}]_i$ in the dendrites and in the somatic submembrane compartment were estimated to range between 0.5 and 1.5 μM. A detailed kinetic analysis is presented in Fig. 4. The schematic drawing in *Right Lower* indicates the somatic (regions a and b) and dendritic regions from which fluorescence was measured; the dotted line indicates the position of the laser beam in the line-scanning mode.

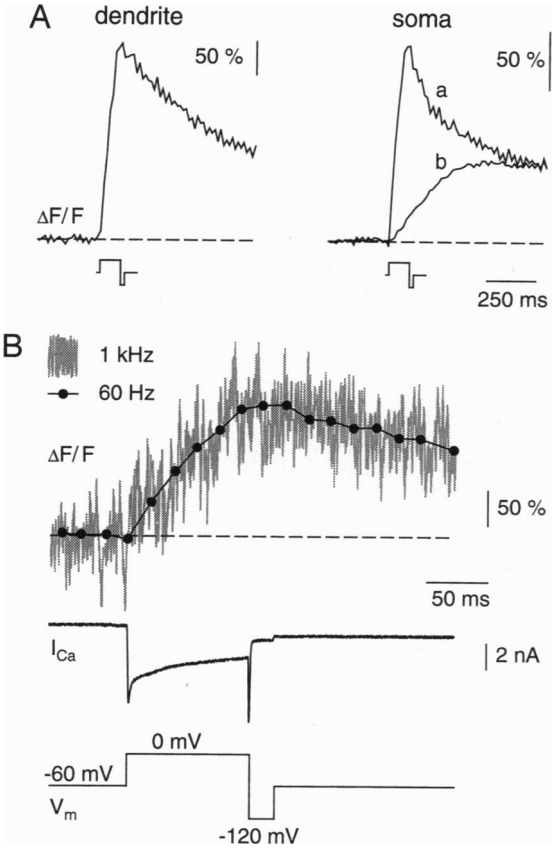

FIG. 4. Time course of Ca^{2+} signals in selected subcellular regions in response to a depolarizing pulse. Data were derived from the experiment of Fig. 3. Fluorescence signals were collected in regions indicated in Fig. 3 *Right Lower*. (*A*) Comparison of Ca^{2+} transients recorded in the dendrite (*Left*), the submembrane somatic shell (*Right*, trace a) and the central somatic region (*Right*, trace b). (*B*) Comparison of Ca^{2+} transients measured with two different acquisition rates in the submembrane somatic shell. The solid trace was derived from deinterlaced video images (trace a in *A* on an expanded time scale); the gray trace was derived from a line-scan experiment obtained within the same submembrane somatic region (Fig. 3). Note the similar time course of the fluorescence recordings obtained at 60 Hz and 1 kHz, respectively. The middle trace shows the Ca^{2+} current (I_{Ca}) recording corresponding to the fluorescence signals shown in Figs. 3 and 4. To avoid possible voltage escape, a short hyperpolarizing pulse (20 ms) was routinely applied after the depolarizing pulse (see bottom trace).

insufficient spatial resolution, the peripheral ring of high $[Ca^{2+}]_i$ was not detected in nonconfocal measurements of $[Ca^{2+}]_i$ (Fig. 1 and refs. 2, 4, and 6–10). CF-induced Ca^{2+} signals either reflect Ca^{2+} influx through voltage-gated Ca^{2+} channels or Ca^{2+} influx amplified by Ca^{2+}-induced Ca^{2+} release from internal stores (13). In Cs^+-tetraethylammonium-loaded cells, the $[Ca^{2+}]_i$ elevation underneath the surface membrane had a monotonic rise with no indication of a secondary component and reached a maximum at the end of the depolarization. It appears, therefore, that under these experimental conditions, Ca^{2+} signals induced by membrane depolarization and CF stimulation merely reflect Ca^{2+} influx through voltage-gated Ca^{2+} channels. The results further suggest that Ca^{2+} channels in the soma attain a density comparable to that in the dendrites. Indeed, in Cs^+-tetraethylammonium-loaded cells, Ca^{2+} transients measured underneath the membrane surface were similar to those detected in the proximal dendrite (Fig. 4*A*).

The finding of large somatic $[Ca^{2+}]_i$ gradients that persisted for several hundred milliseconds emphasizes the point that the diffusion of Ca^{2+} ions in cerebellar Purkinje neurons is effectively restricted. Similar $[Ca^{2+}]_i$ gradients have been observed in a number of cells, including chromaffin cells (20, 21), bullfrog sympathetic neurons (22), frog skeletal muscle fibers (23), and pancreatic acinar cells (24). Restricted diffusion of Ca^{2+} may result from its binding to immobile or slowly mobile buffers (25). Binding to mobile buffers, on the other hand, would speed up the diffusive transport of Ca^{2+} (25). Calcium Green-1 and -5N are mobile buffers and, therefore, $[Ca^{2+}]_i$ gradients in our experiments may dissipate faster than in nondialyzed cells. The Ca^{2+} transient in the subplasmalemmal somatic shell decayed biphasically. The fast component, with a time constant of ≈0.1 s, at least partially reflects diffusion of Ca^{2+} to more central somatic sites. The slow component, with a time constant of ≈0.8 s, is likely to be due to Ca^{2+} removal, via Ca^{2+} pumps and Na^+–Ca^{2+} exchange, in concert with the interaction of Ca^{2+} with high-affinity endogenous buffers, such as calbindin (26). In dendrites, the fast component was not resolved, and $[Ca^{2+}]_i$ decayed monophasically with a time constant of ≈0.7 s, which was similar to the slower time constant measured in the soma.

Our experiments clearly indicate that the surface-to-volume ratio is a major determinant in the Ca^{2+} signal pattern in various cellular compartments. However, the results do not rule out that other factors may also contribute to the heterogeneous Ca^{2+} signals during CF activity. The peak of the CF-induced Ca^{2+} transient in the subplasmalemmal somatic shell (Fig. 2) was smaller than that in dendritic shells (Fig. 1). This difference may arise from the presence of a prominent K^+ conductance in the soma but not in the dendrites. The finding that in the virtual absence of K^+ currents—i.e., in Cs^+-tetraethylammonium-dialyzed cells—the size of the Ca^{2+} transients in the subplasmalemmal somatic shell approached those recorded in dendritic locations (Fig. 4*A*) supports this idea.

Ca^{2+} acting within restricted areas is likely to have specific functions for various cellular processes, including regulation of electrical activity and induction of synaptic plasticity. The results presented here show that in Purkinje neurons, even a single CF response causes clear Ca^{2+} influx across the somatic membrane (Fig. 2*B*). Because an increase in postsynaptic $[Ca^{2+}]_i$ is required for potentiation of γ-aminobutyric acid-mediated whole-cell current responses (19), the Ca^{2+} entry through somatic voltage-gated Ca^{2+} channels provides the link between CF activity and the induction of rebound potentiation of somatic inhibitory synapses (4).

We thank N. Wilhelm for excellent technical help. This work was supported by grants from the Deutsche Forschungsgemeinschaft (SFB 246) and the Bundesministerium für Forschung und Technologie.

1. Bliss, T. V. P. & Collingridge, G. L. (1993) *Nature (London)* **361,** 31–39.
2. Konnerth, A., Dreessen, J. & Augustine, G. J. (1992) *Proc. Natl. Acad. Sci. USA* **89,** 7051–7055.
3. Sakurai, M. (1990) *Proc. Natl. Acad. Sci. USA* **87,** 3383–3385.
4. Kano, M., Rexhausen, U., Dreessen, J. & Konnerth, A. (1992) *Nature (London)* **356,** 601–604.
5. Eilers, J., Augustine, G. & Konnerth, A. (1995) *Nature (London)* **373,** 155–158.
6. Ross, W. N. & Werman, R. (1987) *J. Physiol. (London)* **389,** 319–336.
7. Sugimori, M. & Llinás, R. (1990) *Proc. Natl. Acad. Sci. USA* **87,** 5084–5088.
8. Tank, D. W., Sugimori, M., Connor, J. A. & Llinás, R. R. (1988) *Science* **242,** 773–777.
9. Miyakawa, H., Lev-Ram, V., Lasser-Ros, N. & Ross, W. N. (1992) *J. Neurophysiol.* **68,** 1178–1189.
10. Ross, W. N., Lasser-Ross, N. & Werman, R. (1990) *Proc. R. Soc. London B* **240,** 173–185.
11. Hillman, D., Chen, S., Cherksey, B., Sugimori, M. & Llinás, R. R. (1991) *Proc. Natl. Acad. Sci. USA* **88,** 7076–7080.

12. Usowicz, M. M., Sugimori, M., Cherksey, B. & Llinás, R. (1992) *Neuron* **9,** 1185–1199.
13. Llano, I., DiPolo, R. & Marty, A. (1994) *Neuron* **12,** 663–673.
14. Konnerth, A., Llano, I. & Armstrong, C. M. (1990) *Proc. Natl. Acad. Sci. USA* **87,** 2662–2665.
15. Llano, I., Marty, A., Armstrong, C. M. & Konnerth, A. (1991) *J. Physiol. (London)* **434,** 183–213.
16. Eilers, J., Schneggenburger, R. & Konnerth, A. (1995) in *Single Channel Recording*, eds. Sakmann, B. & Neher, E. (Plenum, New York), 2nd Ed., pp. 213–229.
17. Kano, M., Garaschuk, O., Verkhratsky, A. & Konnerth, A. (1995) *J. Physiol. (London)* **487,** 1–16.
18. Vincent, P., Armstrong, C. M. & Marty, A. (1992) *J. Physiol. (London)* **456,** 453–471.
19. Llano, I., Leresche, N. & Marty, A. (1991) *Neuron* **6,** 565–574.
20. Neher, E. & Augustine, G. J. (1992) *J. Physiol. (London)* **450,** 273–301.
21. O'Sullivan, A., Cheek, T., Moreton, R., Berridge, M. & Burgoyne, R. (1989) *EMBO J.* **8,** 401–411.
22. Hernández-Cruz, A., Sala, F. & Adams, P. (1990) *Science* **247,** 858–862.
23. Monck, J. R., Robinson, I. M., Escobar, A. L., Vergara, J. L. & Fernandez, J. M. (1994) *Biophys. J.* **67,** 505–514.
24. Kasai, H., Li, Y. & Miyashita, Y. (1993) *Cell* **74,** 669–677.
25. Zhou, Z. & Neher, E. (1993) *J. Physiol. (London)* **469,** 245–273.
26. Chard, P., Bleakman, D., Christakos, S., Fullmer, C. & Miller, R. (1993) *J. Physiol. (London)* **472,** 341–357.